THEORETICAL STUDIES ON STEADY-STATE FIBRE PULL-OUT

X. Zhang, H.-Y. Liu and Y.-W. Mai

Centre for Advanced Materials Technology, Department of Mechanical and Mechatronic Engineering, University of Sydney, NSW 2006, Australia

SUMMARY: An improved theoretical model has been developed to study the mechanics of a steady-state fibre pull-out test. With only a few assumptions, the solutions of the stress field satisfy all equilibrium equations, boundary conditions and continuity at the fibre/matrix. As distinct from previous work, the effect of pull-out rate is taken into account in the interfacial friction and debonding. Numerical results of the stress distribution in both bonded and debonded regions are given for a typical carbon/epoxy composite. Applied stress (load)-displacement curves of a fibre pull-out process are obtained by computer simulation.

KEYWORDS: steady-state fibre pull-out, rate-dependent friction, stress field, interface debonding, frictional sliding, local-strain criterion.

INTRODUCTION

Mechanical properties of fibre composites are highly dependent on the integrity of the fibre/matrix interface. Interface debonding and post-debonding friction are two important mechanisms of energy absorption during the failure of a composite. Either high strength or high toughness, or both, of composite materials can be achieved by modifying the interface properties. A comprehensive treatment of engineered interfaces in fibre-reinforced composites is given by Kim and Mai [1]. Over the past several decades, extensive experimental methods have been successfully developed and carried out to investigate the effect of interface on the mechanical behaviour of its composites. Among these tests, the single fibre pull-out test is one of the most powerful tools because of its simplicity and versatility. The load-displacement curve obtained from the test can be used both to determine the interface properties and to study the fracture propagation of a fibre-bridged crack in a fibre composite. To provide a theoretical basis for the single fibre pull-out test, several models have been presented to study its stress field, interface debonding and frictional sliding process [2-5]. But in those previous theoretical models, an important factor, fibre pull-out rate, has not been considered in their analyses. Therefore, all results of the stress transfer, interface debonding and frictional sliding process are rate-independent.

In a fibre pull-out test, the pull-out rate has been found having an important effect on the debonding and frictional sliding processes [6, 7]. The applied pull-out stress is a decreasing function of the pull-out rate. Even in a steady-state fibre pull-out process, a difference of the

pull-out load can also be found between different pull-out rates. This fact cannot be explained by those previous analyses.

The purpose of this paper is to develop theoretical and numerical analyses for a steady-state fibre pull-out test including the effects of pull-out rate. In the theoretical model, the friction in the debonded interfaces is determined by an "extended Columob's law", of which the friction coefficient is rate-dependent. The criterion of the interface debonding is given by a local-shear strain criterion, in which, the critical shear strain depends on the debonding velocity. With few assumptions, the stress distributions in the fibre, matrix and interface are obtained. Computer simulations of the fibre pull-out tests have been presented to illustrate the effects of the pull-out rate on the whole pull-out process.

BASIC EQUATIONS

1. Stress Field

A mechanics model of a single fibre pull-out test is shown in Fig. 1. A fibre with a radius *a* is located at the centre of a coaxial cylindrical matrix with an outer radius *b*. An initial debonded region of length *l* is present at the fibre loading end. The length of the fibre is *L*.

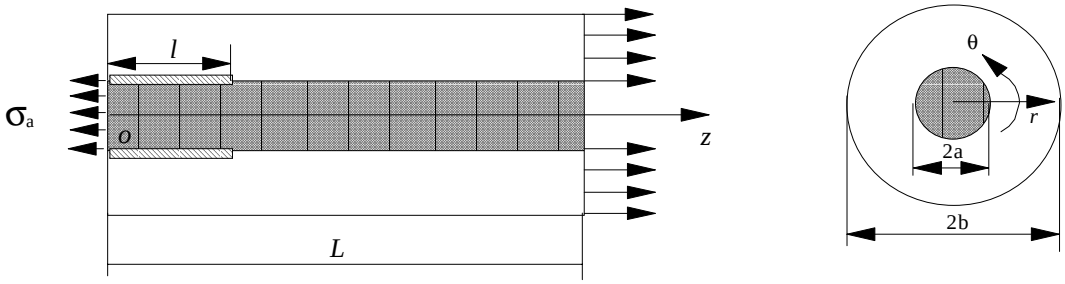

Fig.1 Mechanics model of a fibre pull-out specimen with a partial debonded interface.

In the following analysis, σ is axial stress, τ is shear stress and *u* is displacement. Subscripts *f*, *m* and *i* denote fibre, matrix and interface, respectively. Superscripts *z*, *r* and θ refer to the coordinates. The equilibrium between the axial stresses and interfacial shear stresses can be expressed as

$$\frac{d\sigma_f^z(z)}{dz} = -\frac{2}{a}\tau_i(z) \tag{1}$$

$$\frac{d\sigma_m^z(z)}{dz} = \frac{2\gamma}{a}\tau_i(z) \tag{2}$$

$$\gamma = \frac{a^2}{b^2 - a^2} \tag{3}$$

where, the axial stresses of the fibre and matrix are assumed *z* functions only. From Ref. 2, the hoop and radial stresses of the fibre are

$$\sigma_f^r(z) = \sigma_f^\theta(z). \tag{4}$$

The outer boundary conditions of the fibre/matrix cylinder are

$$\sigma_m^r(b,z) = 0, \qquad \tau_m^{rz}(b,z) = 0 \quad . \tag{5}$$

In the bonded region ($l \le z \le L$), the continuity of axial and radial deformations at the interface requires that

$$u_m^r(a,z) = u_f^r(a,z), \qquad u_m^z(a,z) = u_f^z(a,z). \tag{6}$$

Substituting Eqns 1-6 into the general equations of equilibrium, relationship of displacement, strain and stress [8], the differential equation of the fibre axial stress can be obtained as

$$\frac{d^2\sigma_f^z(z)}{dz^2} - A_1\sigma_f^z(z) = A_2\sigma_a \tag{7}$$

where A_1 and A_2 are parameters related to the fibre/matrix materials and sizes. Because of the limitation of the paper length, the derivation of all equations in this paper and corresponding parameters, such as A_1, A_2, are given elsewhere [9, 10].

In the debonded region ($0 \le z \le l$), the interfacial shear stress is determined from an extended Columob's friction law, that is

$$\tau_i(z) = -\mu[q_i(z) + q^0] \tag{8}$$

in which, q_i, q^0 are radial stresses at the interface arising from a Poisson contraction and an initial thermal mismatch, respectively. μ is the rate-dependent friction coefficient and given by [11]

$$\mu(v_0) = \mu_d + (\mu_s - \mu_d)\exp[-(\frac{v_0}{v_1})^p] \quad . \tag{9}$$

In Eqn 9, v_0 is the pull-out rate and μ_d, μ_s, v_1, p are material parameters. The continuity condition at the debonded region is

$$u_f^r(a,z) = u_m^r(a,z) \tag{10}$$

Combining Eqns 1-5, Enqs 8-10 together with the basic equations of elasticity theory [8], the differential equation for the fibre axial stress in the debonded region is given by [9,10]

$$\frac{d^2\sigma_f^z(z)}{dz^2} + B_1\frac{d\sigma_f^z(z)}{dz} - B_2\sigma_f^z(z) = B_3(\overline{\sigma}) \tag{11}$$

in which, parameters B_1, B_2 and $B_3(\overline{\sigma})$ are given in Ref 9.

As shown in Fig 1, the boundary conditions at the fibre end and the boundary between the bonded and debonded regions are

$$\sigma_f^z(0) = \sigma_a, \qquad \sigma_f^z(l) = \sigma_d, \qquad \sigma_f^z(L) = 0 \tag{12}$$

where, σ_d is denoted as the crack tip debond stress.

In the debonded interface, the frictional shear stress only occurs in the region where the fibre and matrix contact each other. Therefore, the equilibrium between the interfacial shear stress and axial stress (Eqns 1, 2) can be satisfied only when the sum of the interfacial radial stress is compressive. An additional condition, which ensures that the fibre and matrix are in contact at the interface, must be applied, that is

$$q_i(z) + q^0 \le 0 \quad . \tag{13}$$

At the loading end (z=0), the fibre axial stress reaches the maximum value and the matrix axial stress is zero. The maximum interfacial radial stress q_i (in tension) caused by Poisson's effect occurs at the loading end. Therefore, Eqn. 13 can be written at the critical value

$$q_i(0) + q^0 = 0 \tag{14}$$

Solving Eqns 7 and 11 with the boundary conditions, Eqns 12 and 14, leads to the solutions of the fibre axial stress in the bonded region ($l \le z \le L$):

$$\sigma_f^z(z) = k_1^b \sinh(\lambda z) + k_2^b \cosh(\lambda z) - \frac{A_2}{A_1}\sigma_a \quad , \tag{15}$$

and in the debonded region ($0 \le z \le l$):

$$\sigma_f^z(z) = k_1^d \exp(\lambda_1 z) + k_2^d \exp(\lambda_2 z) - \frac{B_3(\overline{\sigma})}{B_2}. \tag{16}$$

The crack tip debond stress σ_d is

$$\sigma_d = \frac{\dfrac{\xi q^0}{B_2 C_1}\Psi_1(l) + \sigma_a \Psi_2(l)}{\lambda_1 - \lambda_2}. \tag{17}$$

The parameters in Eqns 15-17 are given in Ref 9, 10.

2. Interface debonding

Considering interface debonding as a mode-II adhesive crack, a local-shear strain criterion [12] is used as the interface debond criterion. That is

$$\gamma_t^c(v_d) = \gamma_t^c(0) - t_1[1 - \exp(-t_2 v_d)] \tag{18}$$

where, $\gamma_t^c(0)$ represents a static critical shear strain; t_1 and t_2 are material parameters; v_d is the debonding velocity and can be given by [10]

$$v_d \approx \frac{\Delta l}{\Delta u_f^z} v_0 \ . \tag{19}$$

The interfacial shear strain at the crack tip is [8]

$$\gamma_l^{rz} = \frac{2(1+\nu_m)\tau_i}{E_m} \tag{20}$$

in which, E_m and ν_m are Young's modulus and Poisson ratio of the matrix, respectively. The interface debond occurs when the shear strain at the crack tip reaches the critical value. From Eqns 1 and 15, the interface debond criterion can be given by

$$-\frac{a\lambda(1+\nu_m)}{E_m}[k_1^b \cosh(\lambda l) + k_2^b \sinh(\lambda l)] = \gamma_t^c(v_d)\,. \tag{21}$$

3. Frictional sliding

After the interface has been fully debonded, the fibre is pulled out with a frictional sliding process. A mechanics model of the frictional sliding is shown in Fig. 2.

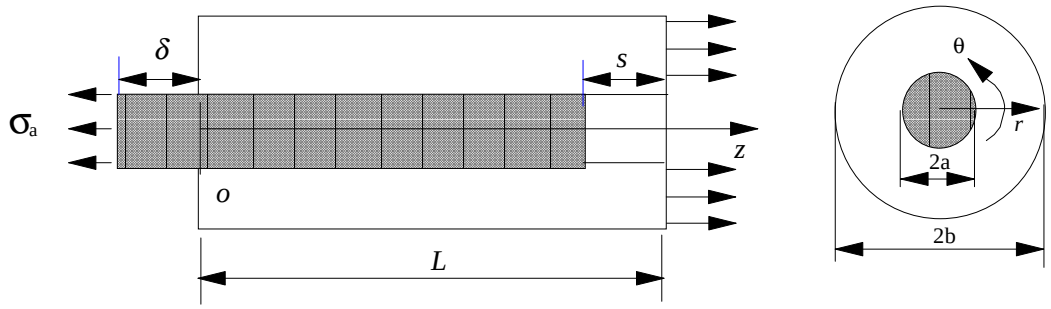

Fig.2 Mechanics model of a fibre pull-out specimen subjected to frictional sliding.

The boundary conditions at the two fibre ends are

$$\sigma_f^z(0) = \sigma_a, \qquad \sigma_f^z(L-s) = 0\,. \tag{22}$$

From the solution of the debonded region, Eqn 16, the fibre axial stress during the frictional sliding is

$$\sigma_f^z(z) = k_1^f \exp(\lambda_1 z) + k_2^f \exp(\lambda_2 z) - \frac{B_3(\bar{\sigma})}{B_2} \tag{23}$$

in which, the parameters are also given in Ref 10.

4. Fibre axial displacement

In a fibre pull-out test, the fibre is progressively pulled out experiencing three different stages: elastic deformation with a fully bonded interface (S-I); elastic deformation with a partial debonded interface (S-II); and elastic deformation plus frictional sliding with a fully debonded interface (S-III). From elasticity theory [8], the relationship between the fibre axial strain (ε_f^z), axial displacement and the stresses is

$$\varepsilon_f^z = \frac{du_f^z}{dz} = \frac{1}{E_f}[\sigma_f^z - \nu_f(\sigma_f^r + \sigma_f^\theta)] \tag{24}$$

where, ν_f is the Poisson ratio of the fibre. Using the stress field obtained in the previous sections (also see Ref 10), the displacement at the fibre end (see Fig. 2), δ, versus applied stress, σ_a, can be derived for three stages, these are

$$\delta = -\frac{1}{E_f}\{\zeta_1[k_1^b - k_1^b\cosh(\lambda L) - k_2^b\sinh(\lambda L)] - \zeta_2\sigma_a L\} \qquad \text{(S-I)} \tag{25}$$

$$\delta = -\frac{1}{E_f}\{k_1^d[1-\exp(\lambda_1 l)](\frac{1}{\lambda_1} - \frac{a\nu_f}{\mu}) + k_2^d[1-\exp(\lambda_2 l)](\frac{1}{\lambda_2} - \frac{a\nu_f}{\mu}) + \frac{B_3}{B_2}l\} - u^{bd}$$

$$u^{bd} = \frac{1}{E_f}\{\zeta_1[k_1^b(\cosh(\lambda l) - \cosh(\lambda L)) + k_2^b(\sinh(\lambda l) - \sinh(\lambda L))] + \zeta_2\sigma_a(l-L)\}$$

(S-II) (26)

$$\delta \approx s \qquad \text{(S-III)} \tag{27}$$

In Eqn 27, the elastic deformation is neglected since it is much smaller than the frictional sliding. All parameters in these equations are given in Ref 10.

5. Numerical examples

Table 1 Fibre, matrix and interface characteristics [3]

Fibre	Young's modulus, E_f (GPa)	230
	Poisson's ratio, ν_f	0.2
	Radius, a (mm)	0.003
Matrix	Young's modulus, E_m (GPa)	3
	Poisson's ratio, ν_m	0.4
	Radius, b (mm)	1.0
Interface	Residual clamping stress, q^0 (MPa)	-10.0

Numerical examples are given for a carbon/epoxy model composite, of which the material properties are given in Table 1. The parameters in the rate-dependent friction model (Eqn 9) are given by [7]: μ_d=0.95, μ_s=1.3, v_1=1 mm/min and p=2. The parameters in debond criterion (Eqn 18) are taken as [12]: t_1=0.026, t_2=0.0028 and $\gamma_t^c(0)$ =0.056.

Computer simulation results of the debonding process are given in Fig. 3. The applied stress versus the debonding length is calculated by Eqns 18, 19 and 21. The pull-out rate, v_0, are given as $0.01v_1$ (——), $0.1v_1$ (— —) and v_1 (------). The lengths of the fibre are taken as 0.1 mm and 0.5 mm, respectively. It is shown that, for a longer fibre, the applied stress increases with debonding length until it is approximately 0.4 mm. This implies that stable debonding occurs during the test. But when the fibre is short, L=0.1 mm, no stable debonding can be seen. It is also shown that the fibre pull-out rate significantly affect the debonding process. From Eqns 9 and 18, both the friction coefficient and the critical shear strain decrease with increasing pull-out rate. Therefore, the resistance to debonding decreases with pull-out rate. As a result, in Fig. 3, when the pull-out rate is higher, the applied stresses for both initial debonding and debond crack growth are lower.

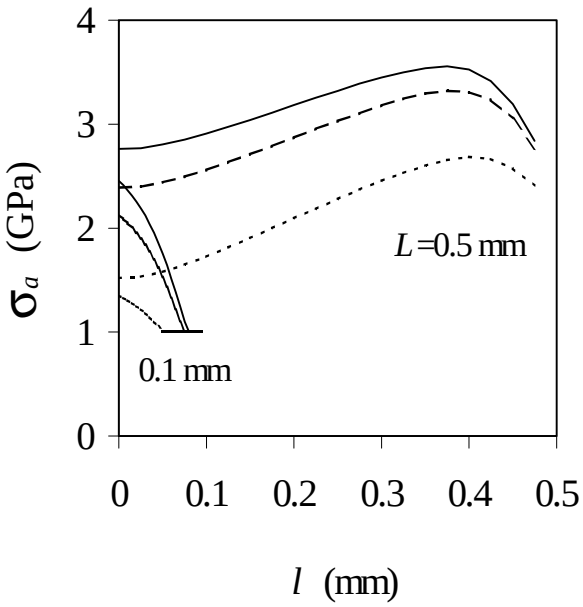

Fig. 3. Plots of applied stress versus debonding length, where the pull-out rates, v_0, are $0.01v_1$ (——), $0.1v_1$ (— —) and v_1 (------).

Distributions of the fibre axial stress and interfacial shear stress along the fibre length are given in Figs. 4a and 4b, where the debonding length is half the fibre length. The applied stresses for the three curves are obtained from Fig.3 and they are: 3.32 GPa (v_0=$0.01v_1$), 3.03 GPa (v_0=$0.1v_1$) and 2.28 GPa (v_0=$1v_1$), respectively. In Fig. 4a, at the same debonded length, the fibre axial stress decreases with increasing pull-out rate. In Fig. 4b, the interfacial shear stresses in the debonded region ($0 \le z \le 0.25$ mm), are very small and rise significantly at the debonding crack tip, z=l=0.25 mm. Since the critical shear strain reduces with debond velocity. The shear stresses at the crack tip (z=l^+) reduce with pull-out rate. It should be mentioned here, from the rate-dependent friction model, Eqn 9, the friction coefficient decreases with pull-out rate. Generally, the interfacial friction should decrease with pull-out rate in the debonded region. But, in Fig.4b, the interfacial shear stress of a high pull-out rate is greater than that of a low pull-out rate. This can be explained by the fact that interfacial friction is determined by two factors: friction coefficient and interfacial radial compression (Eqn 8). From Fig. 4a, the fibre axial stress of a high pull-out rate is much lower than that of a low pull-out rate. Under a high pull-out rate, the radial stress from Poisson contraction, q_i (in tension), is low. Therefore, the total interfacial compression caused by both thermal residual stress (compression) and Poisson contraction (tension) are high. As a result, in some cases (particularly, when q^0 is low), the effect of pull-out rate on interfacial friction may be reduced.

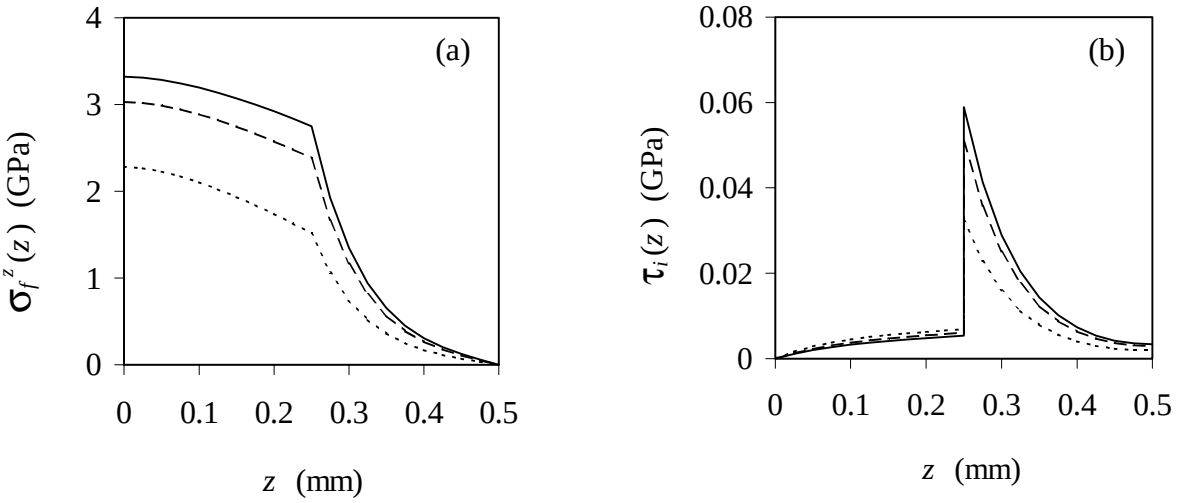

Fig. 4. Distributions of (a) fibre axial stress, (b) interfacial shear stress along the fibre length with a partially debonded interface, where, L=0.5 mm, l=0.25 mm and the pull-out rates, v_0, are $0.01v_1$ (——), $0.1v_1$ (— —) and v_1 (------).

Computer simulations of the applied stress (load)-displacement curves are given in Fig. 5. The whole process is made up of three stages: elastic deformation with a fully bonded interface (S-I); elastic deformation with a partially debonded interface (S-II); and frictional sliding with a fully debonded interface (S-III). The displacements of the fibre in the first (S-I) and second (S-II) stages are much smaller than that in the third stage (S-III). In Fig. 5, therefore, the whole pull-out curves are separated into two parts: (a) for S-I and S-II and (b) for S-III. It is shown that, in the first stage, all three curves increase simultaneously with applied stress. In the second stage, the effect of the pull-out rate on both interface debond initiation and propagation are significant. After the interface has been fully debonded, the difference between the curves: v_0=$0.01v_1$ and $0.1v_1$ is invisible.

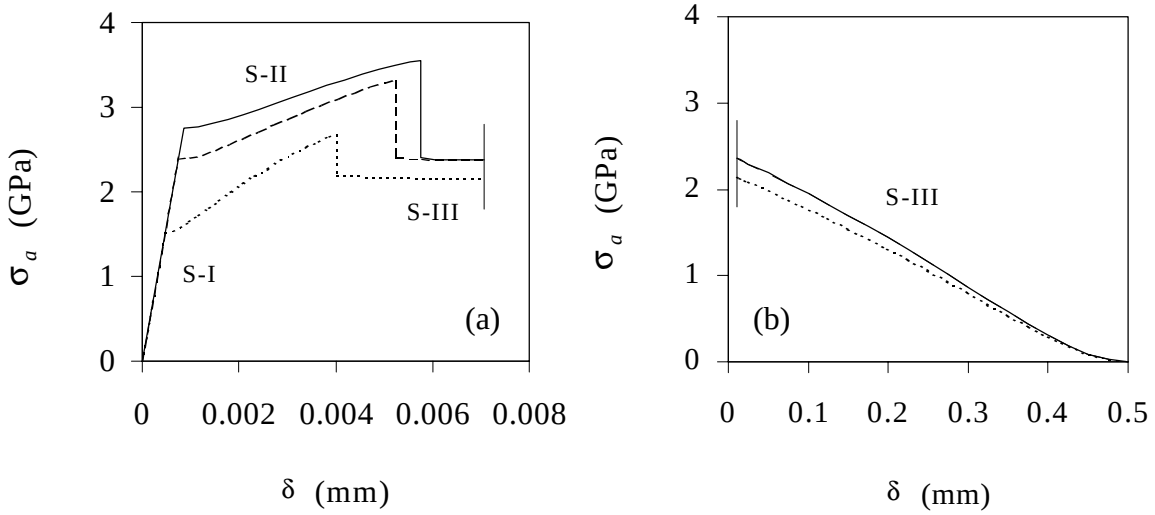

Fig. 5 Computer simulation of applied stress-displacement curves of fibre pull-out test, where the fibre length is 0.5 mm and the pull-out rates are $0.01v_1$ (——), $0.1v_1$ (— —) and v_1 (------).

CONCLUSION

Theoretical analysis of a steady-state fibre pull-out test has been presented. With a minimum number of assumptions, the stress fields in both bonded and debonded regions can be obtained. The fibre pull-out rate is considered in the analyses of both interfacial friction and debonding. Numerical examples of the stress distribution, interface debonding and frictional sliding processes show that the effects of the fibre pull-out rate are important in the whole pull-out test.

ACKNOWLEDGMENT

The authors would like to thank the Australia Research Council (ARC) for the continuing support of this project. Hongyuan Liu is supported by an ARC Postdoctoral Fellowship tenable at the University of Sydney and Xi Zhang by an Overseas Postgraduate Research Scholarship (OPRS).

REFERENCES

1. *Engineered interfaces in fibre-reinforced composites*, by Kim J.-K. and Mai, Y.-W., Elsevier Science Publications Ltd., Oxford, 1998, pp. 401.

2. Gao, Y.-C., Mai, Y.-W. and Cottrell, B., "Fracture of fibre-reinforced materials", *ZAMP*, **39,** 1988, pp. 550-572.

3. Zhou, L.-M., Kim, J.-K. and Mai, Y.-W., " Interfacial dbonding and fibre pull-out stresses: Part II. A new model based on the fracture mechanics approach", *Journal of Materials Science*", **27**, 1992, pp. 3155-3166.

4. Nairn, J.A. and Liu, Y.C., "Stress transfer into a fragmented, anisotropic fibre through an imperfect interface", *International Journal of Solids and Structures*, **34**, 1997, pp.1255-1281.

5. Hsueh, C.-H., "Interfacial debonding and fibre pull-out stresses of fibre-reinforced composites", *Materials Science and Engineering*, **A123**, 1990, pp. 1-11.

6. Rice, J.R. and Ruina, A.L., "Stabilility of steady frictional slipping", *Journal of Applied Mechanics*, **50,** 1983, pp. 343-347.

7. Tsai, K.-H. and Kim, K.-S., "The micromechanics of fibre pull-out", *Journal of Mechanics and Physics of Solids*, **44**, 1996, pp. 1147-1177.

8. *Theory of elasticity*, third Edition, by Timoshenko, S.P. and Goodier, J.N., McGraw-Hill, New York, 1970.

9. Zhang, X., Liu, H.-Y., Mai, Y.-W. and Diao, X.X., "On steady-state fibre pull-out, Part I: stress field", *Composite Science and Technology*, 1999, submitted.

10. Liu, H.-Y., Zhang, X., and Mai, Y.-W., "On steady-state fibre pull-out, Part II: Computer simulation", *Composite Science and Technology*, 1999, submitted.

11. Povirk, G.L. and Needleman, A., “Finite element simulations of fibre pull-out”, *Journal of Engineering Materials and Technology*, **115**, 1993, pp. 286-291.

12. Chai, H. and Chiang, M.Y.M., “A crack propagation criterion based on local shear strain in adhesive bonds subjected to shear”, *Journal of Mechanics and Physics of Solids*, **44**, 1996, pp. 1669-1689.